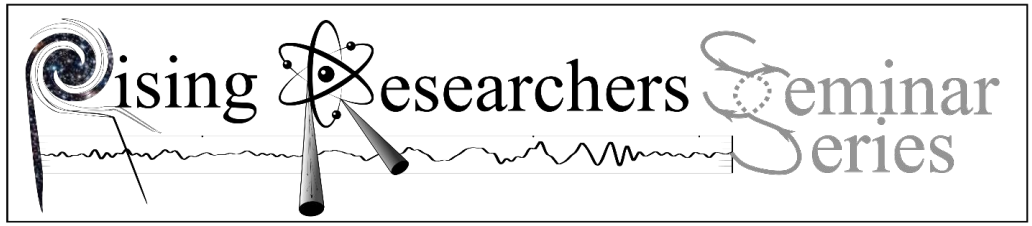

The Rising Researchers Seminar Series is committed to creating an **environment which is welcoming and safe** for all speakers, attendees, organizers, and other affiliated persons, hereinafter ``participants". It is the responsibility of all participants to foster such an environment.

Participants shall **treat each other professionally and respectfully**. Participants shall refrain from any inappropriate behaviour, including discriminatory actions and comments based on individual characteristics such as age, race, ethnicity, sexual orientation, gender identity, gender expression, marital status, nationality, immigration status, political affiliation, ability status, or educational background. Disruptive or harassing behavior will not be tolerated including but not limited to inappropriate or intimidating language and unwelcome jokes or comments.

Violations of this code of conduct should be reported to any member of the executive committee (see About Us page on the website). The Executive committee may also act of their own accord should they notice violations. Sanctions may range from verbal warning, to ejection from the meeting or, in severe cases, partial or total bans from future meetings.

References: This code of conduct is based heavily on that of the INT and the APS. We are also grateful to Roxanne Springer for valuable discussion and guidance.

Towards Real-Time Lattice Simulation of Baryogenesis

Tong Ou

The University of Chicago
tongou@uchicago.edu

Rising Researchers Seminar Series, 11/4/2025

Baryogenesis

There are more baryons than anti-baryons in the Universe:

$$Y_B \equiv \frac{n_B - n_{\bar{B}}}{s} \simeq 0.9 \times 10^{-10}.$$

Two possible scenarios leading to this fact:

- The Universe started from an initial state with $\Delta_B = n_B - n_{\bar{B}} > 0$.
  However, two issues arise: First, we need an extremely fine-tuned initial Δ_B to explain the observed Y_B. Second, inflation would exponentially dilute any amount of initial baryon number.
- The Universe started from a state with $n_B = n_{\bar{B}}$, and generated baryon asymmetry through dynamical processes. This scenario is called **Baryogenesis**.

Sakharov's conditions for baryogenesis A.D.Sakharov, 1967:

1. Baryon number violation
2. C, CP violation
3. Out of thermal equilibrium

Sakharov's conditions

- Baryon number violation — Of course, we are generating baryon number asymmetry.
- C, CP violation

$$\mathrm{C} : L \to \bar{R}, R \to \bar{L}$$

$$\mathrm{CP} : L \to \bar{L}, R \to \bar{R}$$

$$\not{\mathrm{C}}\not{\mathrm{P}} : \quad \Delta_L = n_L - n_{\bar{L}} \neq 0, \quad \Delta_R = n_R - n_{\bar{R}} \neq 0$$

$$\not{\mathrm{C}} : \quad \Delta_L \neq -\Delta_R \;\Rightarrow\; \Delta_L + \Delta_R \neq 0$$

- Out of thermal equilibrium — Baryons and anti-baryons have equal masses, and thus have equal equilibrium numbers $n_B \sim \exp(-M_B/T)$. If the baryon number violation process occurs in equilibrium, the asymmetry would eventually be washed out.

Electroweak Baryogenesis (EWBG)

Now we focus on a highly motivating mechanism: Baryon asymmetry generated during the electroweak phase transition: $\langle h \rangle : 0 \to v$.

Sakharov's conditions for baryogenesis:

1. Baryon number violation
2. Out of thermal equilibrium
3. C, CP violation

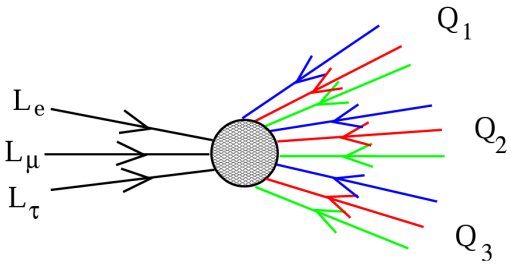

Weak sphaleron, $\Delta B(L) \neq 0$, $\Delta(B - L) = 0$

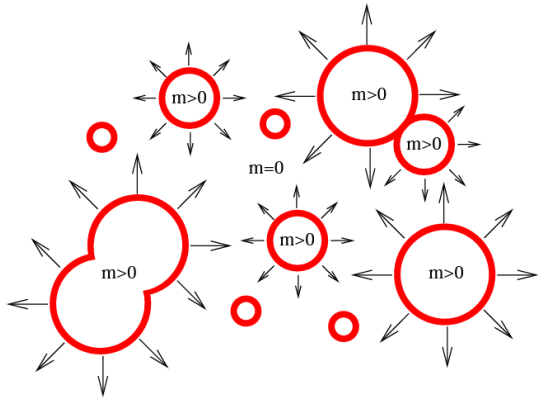

Bubble nucleation during first order EWPT. $m = 0$: symmetric phase, $m > 0$: broken phase.

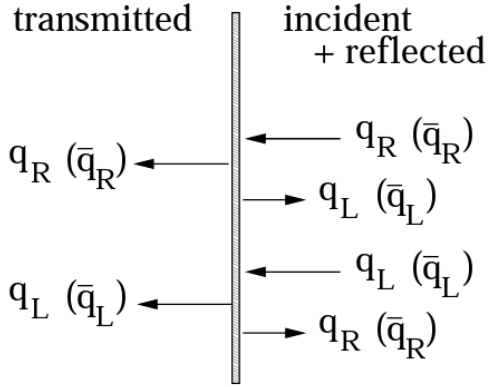

CP-violating scattering of the fermions with the bubble wall. Reflection rates $R_L \neq R_{\bar{L}}$.

CP asymmetry $(n_L - n_{\bar{L}})$ generated through scattering would bias the sphaleron to generate more baryons than anti-baryons.

Electroweak Baryogenesis (EWBG)

We performed a real-time lattice simulation of asymmetry generation through fermion scattering with the bubble wall in 1+1D.

Marcela Carena, Ying-Ying Li, TO, Hersh Singh, 2412.10365

Sakharov's conditions for baryogenesis:

1. Baryon number violation
2. Out of thermal equilibrium
3. C, CP violation

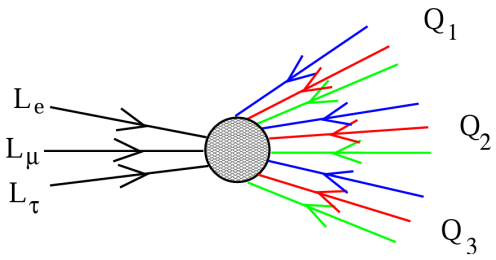

Sphaleron, $\Delta B(L) \neq 0$, $\Delta(B-L) = 0$

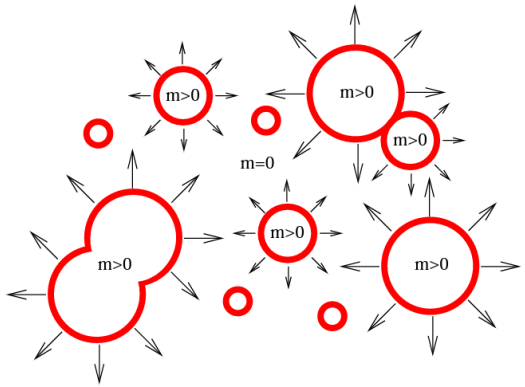

Bubble nucleation during first order EWPT

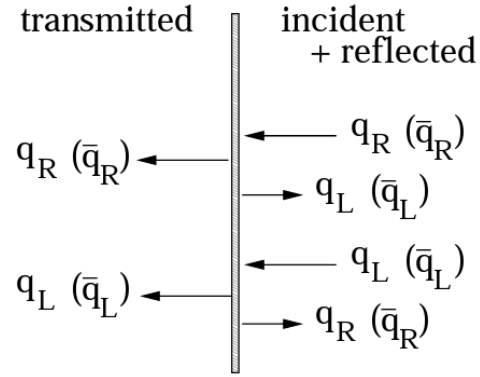

CP-violating scattering of the fermions with the bubble wall. Reflection rates $R_L \neq R_{\bar{L}}$.

- *Why real-time?* — Applicable to non-equilibrium processes.
- *Why lattice?* — To address the uncertainties in the conventional perturbative calculations.

Conventional Calculations of CP Asymmetry

Equation of motion: Dirac equation with a spatially varying complex mass

$$i\partial\!\!\!/\Psi(t,\mathbf{x}) - m(z)P_R\Psi(t,\mathbf{x}) - m^*(z)P_L\Psi(t,\mathbf{x}) = 0.$$

Two perturbative approaches to calculate the CP-violating effects:

- Semi-classical approach based on WKB approximation.
  In the "thick" wall limit, $L_w \gg \lambda \sim 1/T$, the dynamics of the fermion near the bubble wall can be approximated as the WKB ansatz $\Psi \sim e^{-iE_w t + i\int^z p(z')dz'}$. The impact of the bubble wall on the fermion can be described by a classical force (to the leading order of spatial derivatives):

$$F_z = -\frac{(|m|^2)'}{2E_w} + ss_{k_0}\frac{\left(|m|^2\theta'\right)'}{2E_w E_{wz}}$$

  $ss_{k_0} = +1(-1)$ for $L(\bar{L})$, encoding CP violation. The particle distribution near the bubble wall can be solved from the Boltzmann equation

$$(v_g\partial_z + F_z\partial_{k_z})\, f_i = C_i[f_i, f_j, ...]$$

M. Joyce, T. Prokopec, N. Turok, 9410282

J. Cline, M. Joyce, K. Kainulainen, 0006119

Conventional Calculations of CP Asymmetry

Another perturbative approach:

- VEV-insertion approximation: Treat the mass term as perturbation that mixes the left and right-handed components. Calculate the reflection coefficient of the left-handed particle reflected into right-handed R_{LR} as expansion in $m(z)$:

$$R_{LR} = -i \int dz_1 G_R(-z_1)[-m^*(z_1)] G_L(z_1)$$
$$-i \int dz_1 dz_2 dz_3 G_R(-z_3)[-m^*(z_3)] G_L(z_3 - z_2)$$
$$m(z_2) G_R(z_2 - z_1)[-m^*(z_1)] G_L(z_1) + \ldots$$

where $G_{L,R}$ are the Green's functions.

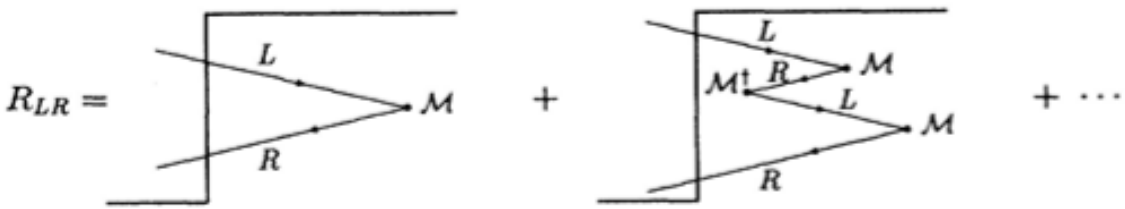

P. Huet, E. Sather, 9404302

P. Huet, A. E. Nelson, 9506477

Conventional Calculations of CP Asymmetry

Limitations of the two approaches:

- Semi-classical approach: Limited to thick wall scenario where quantum effects are negligible.
- VEV-insertion approach: Limited to light mass $m/T \ll 1$, which is invalid near the broken phase for a strong first-order phase transition with $v/T > 1$.

Moreover, numerical calculations found an order-of-magnitude discrepancy between the baryon numbers predicted by the two approaches for typical EWBG models (CK and FH in the plots both refer to the semi-classical approach):

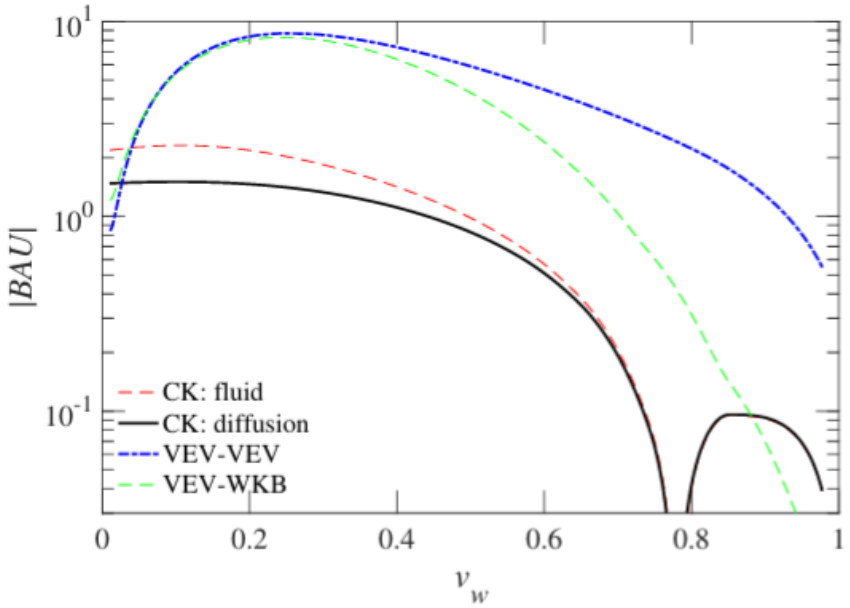

J. Cline, K. Kainulainen, 2001.00568

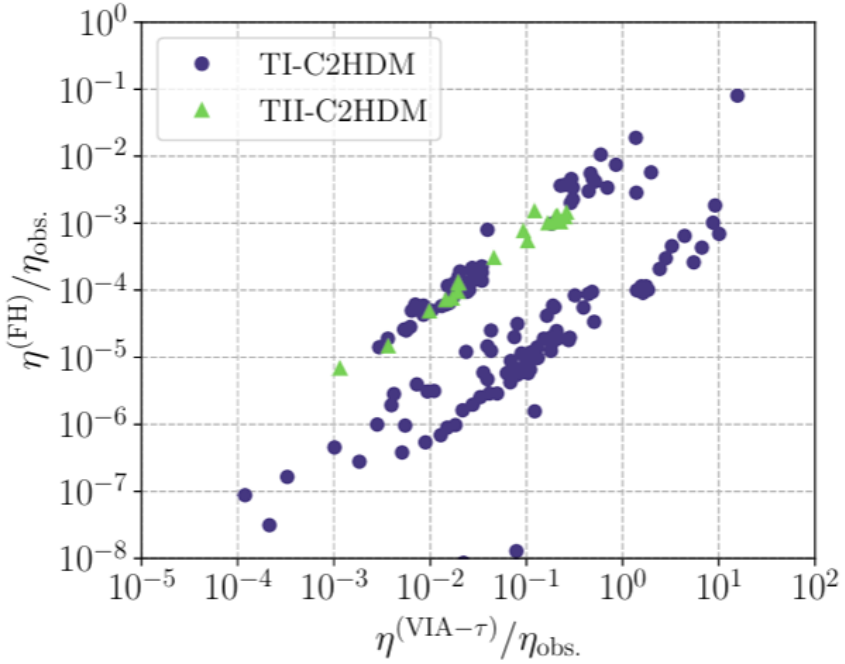

P. Basler, M. Mühlleitner, J. Müller, 2108.03580

Symmetry Breaking by the Complex Mass Term

We use the Hamiltonian formalism. The Hamiltonian of the fermion with a complex mass profile $m(x) = |m(x)|e^{i\theta(x)\gamma^5}$ is given by

$$\mathcal{H} = -i\overline{\psi}\gamma^j\partial_j\psi + |m(x)|\overline{\psi}\left[\cos\theta(x) + i\sin\theta(x)\gamma^5\right]\psi.$$

To discuss what discrete symmetry is broken by this Hamiltonian, we first define charge conjugation as

$$\begin{aligned} C_\epsilon\gamma_\mu C_\epsilon^{-1} &= \epsilon(\gamma_\mu)^T, \quad (\epsilon = \pm) \\ C_\epsilon\gamma_5 C_\epsilon^{-1} &= \eta_5(\gamma_5)^T, \quad \eta_5 = (-1)^{\frac{D}{2}} \end{aligned}$$

The spinors transform as

$$\mathsf{C}_\epsilon : \ \psi \to C_\epsilon\overline{\psi}^T, \quad \overline{\psi} \to \epsilon\psi^T C_\epsilon^{-1}$$

One can check that the kinetic term is invariant under charge conjugation

$$\overline{\psi}\gamma^\mu\partial_\mu\psi \xrightarrow{\mathsf{C}_\epsilon} \epsilon\overline{\psi}(C_\epsilon^{-1}\gamma^\mu C_\epsilon)^T\partial_\mu\psi = \overline{\psi}\gamma^\mu\partial_\mu\psi$$

While the mass term may not be invariant, and a fermion bilinear in general transforms as

$$\overline{\psi}\Gamma\psi \xrightarrow{\mathsf{C}_\epsilon} \overline{\psi}(-\epsilon C_\epsilon^{-1}\Gamma C_\epsilon)^T\psi$$

Symmetry Breaking by the Complex Mass Term

We define parity transformation as

$$\mathsf{P}: \begin{cases} \psi(t,x) \to \kappa\gamma_0\psi(t,-x) \\ \overline{\psi}(t,x) \to \overline{\psi}(t,-x)(\kappa\gamma_0)^\dagger \end{cases}$$

where $\kappa = 1$ or i so that $(\kappa\gamma_0)^2 = 1$.
Again the kinetic term is always invariant under parity transformation, while the fermion bilinear transforms as

$$\overline{\psi}\Gamma\psi \xrightarrow{\mathsf{P}} \overline{\psi}\gamma_0^{-1}\Gamma\gamma_0\psi.$$

The transformations of the fermion bilinears under charge conjugation and parity transformation are summarized as

Γ	1	γ^5	γ^μ	$\gamma^\mu\gamma^5$
C_ϵ	$-\epsilon$	$-\epsilon\eta_5$	-1	η_5
P	1	-1	$(-1)^\mu$	$-(-1)^\mu$

Marcela Carena, Ying-Ying Li, TO, Hersh Singh, 2412.10365
M. Stone, 2009.00518

Symmetry Breaking by the Complex Mass Term

Γ	1	γ^5	γ^μ	$\gamma^\mu\gamma^5$
C_ϵ	$-\epsilon$	$-\epsilon\eta_5$	-1	η_5
P	1	-1	$(-1)^\mu$	$-(-1)^\mu$

The real and imaginary parts of the mass term, $\overline{\psi}\psi$ and $\overline{\psi}\gamma^5\psi$, transform differently in different dimensions [$\eta_5 = (-1)^{\frac{D}{2}}$]:

$$\text{3+1D:}\quad \eta_5 = +1,\ \overline{\psi}\psi \xrightarrow{C_\epsilon P} -\epsilon,\quad \overline{\psi}\gamma^5\psi \xrightarrow{C_\epsilon P} \epsilon$$

$$\text{1+1D:}\quad \eta_5 = -1,\ \overline{\psi}\psi \xrightarrow{C_\epsilon} -\epsilon,\quad \overline{\psi}\gamma^5\psi \xrightarrow{C_\epsilon} \epsilon$$

Therefore, the complex mass term breaks **CP** symmetry in **3+1D**, while breaks **C** symmetry in **1+1D**.

Observables for Symmetry Breaking

Ideal symmetry breaking observables: Vanish in the initial state which is symmetric under C or CP. Evolve to be non-zero as symmetry breaking occurs when the fermion hits the bubble wall

$$\langle \mathcal{O} \rangle_{t=0} = 0 \rightarrow \langle \mathcal{O} \rangle_{t_f} \neq 0$$

$\mathcal{O}$ can be any operator that is odd under the corresponding symmetry.

Γ	1	γ^5	γ^μ	$\gamma^\mu\gamma^5$
C_ϵ	$-\epsilon$	$-\epsilon\eta_5$	-1	η_5
P	1	-1	$(-1)^\mu$	$-(-1)^\mu$

- The chiral charge density $j^0_A \equiv \overline{\psi}\gamma^0\gamma^5\psi$ is CP-odd in 3+1D, and can be used to measure CP asymmetry in 3+1D EWBG.
- The vector charge density (particle number density) $j^0_V \equiv \overline{\psi}\gamma^0\psi$ is C-odd in 1+1D, and will be used to measure C asymmetry generation in the 1+1D simulation in this work.

Evolution Picture

1. Prepare the initial state to be a massless Gaussian wavepacket sitting in the middle of the symmetric phase, far from both the bubble wall and the lattice boundary.
2. Time evolve the system with the operator $U(t, t+dt) = e^{-iHdt}$. Let the wavepacket move towards the bubble wall and scatter with it. Measure the particle (anti-particle) charge density as a function of time:

$$\rho_{n,\pm}(t) = < \Psi_{\pm}(t)|\hat{j}_n^0|\Psi_{\pm}(t) > - < \Omega|\hat{j}_n^0|\Omega >$$

3. To measure symmetry breaking, we perform the procedures above for a pair of identical particle and anti-particle wavepackets individually, and sum up their local charge densities to get the net charge density: $\rho_n(t) = \rho_{n,+}(t) + \rho_{n,-}(t)$.

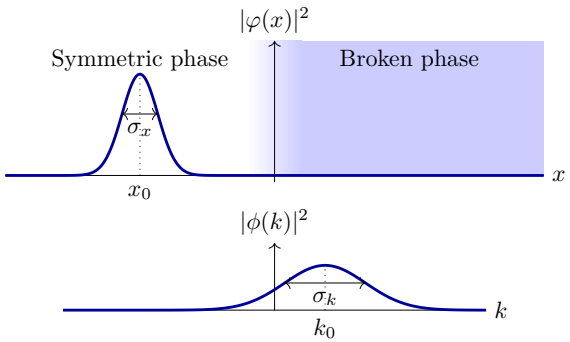

Wavepacket in the position and momentum space

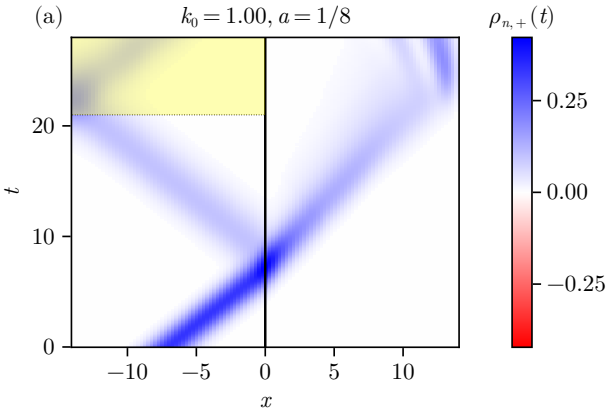

Particle only

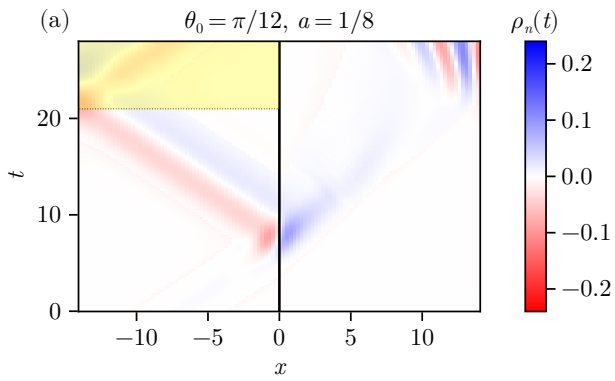

Particle + anti-particle

Lattice Discretization

Continuum Hamiltonian

$$\mathcal{H} = -i\overline{\psi}\gamma^j\partial_j\psi + m\overline{\psi}\psi$$

Naive discretization

$$\psi(x = na) \to \chi_n, \quad \partial_x\psi|_{x=na} \to \frac{\chi_{n+1} - \chi_{n-1}}{2a}$$

Taking periodic boundary condition, the momentum modes can be defined as

$$\chi_k = \frac{1}{\sqrt{N}}\sum_n \chi_n\, e^{-ikna}, \quad k = -\frac{\pi}{a} + j\frac{2\pi}{Na} \quad (j = 1, ..., N)$$

The lattice Hamiltonian

$$H = \sum_k \chi_k^\dagger \begin{pmatrix} -m & -i\frac{\sin ka}{a} \\ i\frac{\sin ka}{a} & m \end{pmatrix} \chi_k = \sum_k \chi_k^\dagger\, H_k\, \chi_k$$

For an eigenstate with energy E,

$$\left(\frac{\sin ka}{a}\right)^2 + m^2 = E^2 \quad \xrightarrow{a\to 0} \quad k^2 + m^2 = E^2$$

while there are only 2 k-modes in the continuum $k = \pm\sqrt{E^2 - m^2}$, there are 4 k-modes in the discrete Hamiltonian $k = \pm k_0, \pm(k_0 + \frac{\pi}{a})$ — Fermion doubling issue.

Lattice Discretization

- Work in the staggered fermion formalism to avoid fermion doubling issue

$$\psi(x) = \begin{pmatrix} \psi_1 \\ \psi_2 \end{pmatrix} \quad \rightarrow \frac{1}{\sqrt{a}} \begin{pmatrix} \chi_{2j-1} \\ \chi_{2j} \end{pmatrix}, \quad j = 1, ..., N/2$$

Taking open boundary condition, the dimensionless discrete Hamiltonian is given by

$$\hat{H} = \sum_{n=1}^{N-1} i \left[\frac{1}{2} + (-1)^n |m_n| \sin\theta_n \right] (\chi_{n+1}^\dagger \chi_n - \chi_n^\dagger \chi_{n+1}) - \sum_{n=1}^{N} (-1)^n |m_n| \cos\theta_n \chi_n^\dagger \chi_n$$

with $m_n \equiv am(an - aN_c)$, $\theta_n \equiv \theta(an - aN_c)$, where N_c is the site of the wall center.

- This Hamiltonian can be mapped to a spin chain by Jordan-Wigner transformation

$$\chi_n = \left(\prod_{s<n} i\sigma_s^z \right) \sigma_n^+, \qquad \chi_n^\dagger = \left(\prod_{s<n} -i\sigma_s^z \right) \sigma_n^-$$

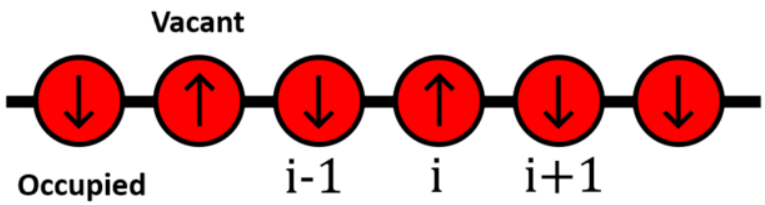

which can be directly implemented on a quantum computer in the future.

Lattice Discretization

- We use the tensor network methods for the numerical simulation — formulate the operators as matrix product operators (MPO), and the quantum states as matrix product states (MPS) ITensor documentation.

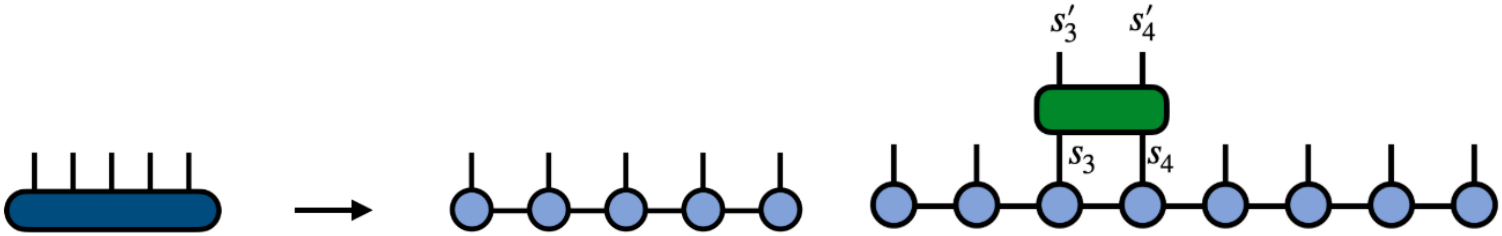

- Time evolution — Trotterization. Decompose the Hamiltonian into the neighboring terms

$$\hat{H} = \sum_{n=1}^{N-1} h_{n,n+1} + h_N, \quad h_N = (-1)^{N+1} |m_N| \cos\theta_N \sigma_N^- \sigma_N^+$$

$$h_{n,n+1} = \left[\frac{1}{2} + (-1)^n |m_n| \sin\theta_n\right] (\sigma_{n+1}^- \sigma_n^+ + \sigma_n^- \sigma_{n+1}^+) - (-1)^n |m_n| \cos\theta_n \sigma_n^- \sigma_n^+$$

then decompose the time evolution operator as

$$e^{-i\hat{H}\hat{\tau}} \approx e^{-ih_{1,2}\hat{\tau}/2} e^{-ih_{2,3}\hat{\tau}/2} \cdots e^{-ih_{N-1,N}\hat{\tau}/2} e^{-ih_N\hat{\tau}}$$
$$e^{-ih_{N-1,N}\hat{\tau}/2} \cdots e^{-ih_{2,3}\hat{\tau}/2} e^{-ih_{1,2}\hat{\tau}/2} + \mathcal{O}(\hat{\tau}^3)$$

Validation

We first examine our algorithm by simulating a fermion wavepacket scattering with a real mass profile:

$$|m(x)| = \frac{m_0}{2}\left[1 + \tanh\left(x/L_w\right)\right] \quad \& \quad \theta(x) = 0$$

In this case, there is a precise analytic prediction of the reflection coefficient, which is defined as the ratio of the reflected particle number $\mathcal{Q}_{t,\pm} = \int_{-\infty}^{0} dx \rho_{\pm}(x,t)$ at the asymptotic limit ($t \to \infty$) to the incident particle number.

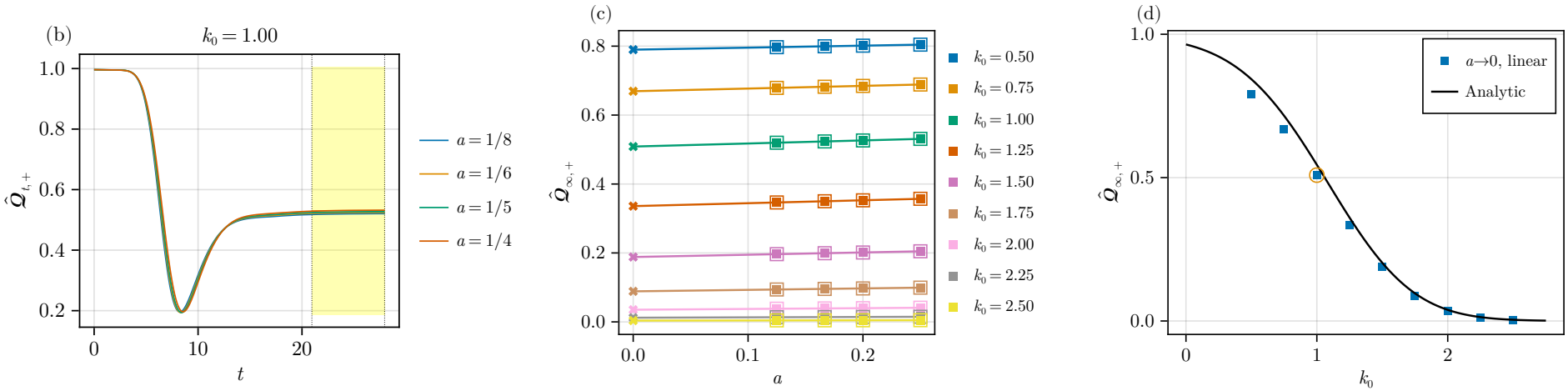

We perform the simulations in a fixed lattice volume $L = 28$ with wall width $L_w = 0.6$ and various lattice spacings a. The asymptotic value $\hat{\mathcal{Q}}_{\infty,+}$ is measured as the mean value of $\hat{\mathcal{Q}}_{t,+}$ in the yellow band of (b). The continuum limits of $\hat{\mathcal{Q}}_{\infty,+}$ agree with the analytic predictions.

Scale Separation

One of the most challenging aspects of these simulations is that we need the wavepacket to be localized in both position and momentum space.

- In the position space, we want the wavepacket to be far away from both boundaries of the symmetric phase ($x \in [-L/2, 0]$):

$$0 \ll |x_0 \pm \sigma_x| \ll \frac{L}{2}$$

- In the momentum space, we want to suppress both negative (left-moving) momentum modes and large momentum modes that are associated with large lattice artifacts (ensure validity of $\sin ka \sim ka$):

$$0 \ll |k_0 \pm \sigma_k| \ll \frac{\pi}{2a}$$

- In practice we choose $x_0 = -L/4$, therefore $\sigma_x \ll L/4$. Using $\sigma_x \sigma_k = 1/2$ for Gaussian distribution, we obtain the following condition for k_0 and σ_k:

$$\frac{\pi}{2a} \gg k_0 \gg \sigma_k \gg \frac{2}{L}.$$

Symmetry Breaking

To simulate charge symmetry breaking, we use the following mass and phase profiles

$$|m(x)| = \frac{m_0}{2}\left[1 + \tanh\left(x/L_w\right)\right], \quad \theta(x) = \frac{\theta_0}{2}\left[1 + \tanh\left(x/L_w\right)\right]$$

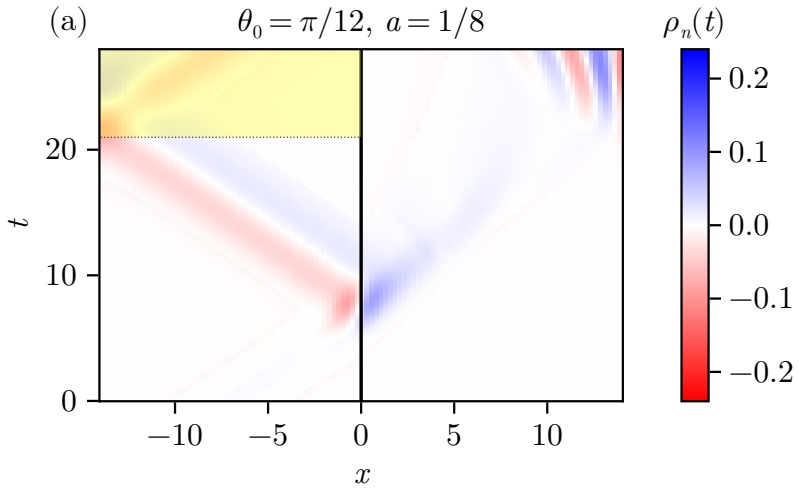

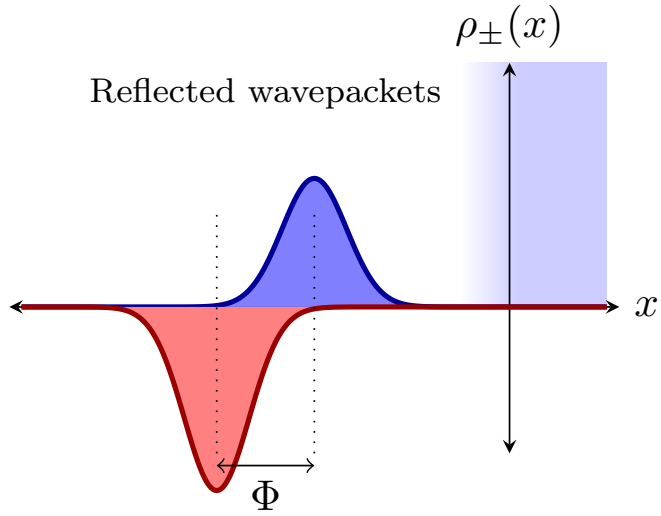

Asymmetries generated in the reflection coefficient $R_\pm(k) = |R_\pm(k)|e^{i\phi_\pm(k)}$:

- Magnitude asymmetry $|R_+(k)| \neq |R_-(k)|$ — measured by the net reflected particle number $\hat{\mathcal{Q}}_\infty \equiv \hat{\mathcal{Q}}_{\infty,+} + \hat{\mathcal{Q}}_{\infty,-}$.
- Phase asymmetry $\phi_+(k) \neq \phi_-(k)$ — measured by the spatial displacement between the particle and anti-particle wavepacket centers $\Phi = \phi'_+(k_0) - \phi'_-(k_0)$.

Magnitude Asymmetry

Again, we run the simulations in a fixed lattice volume $L = 28$ with wall width $L_w = 0.6$, varying lattice spacing a and the phase parameter θ_0 (k_0 is fixed at 1).

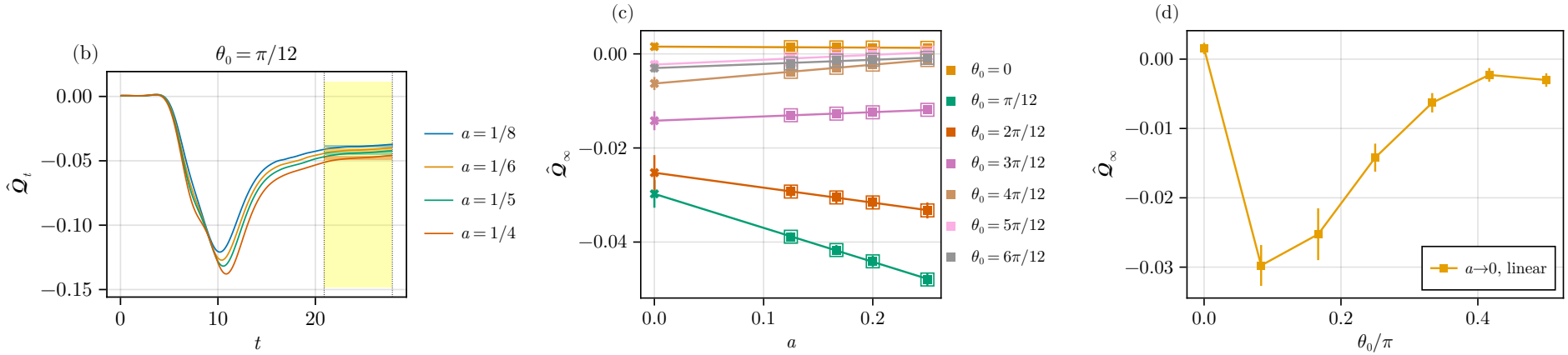

Magnitude asymmetry gets smaller at larger θ_0 — Does it mean smaller asymmetry?

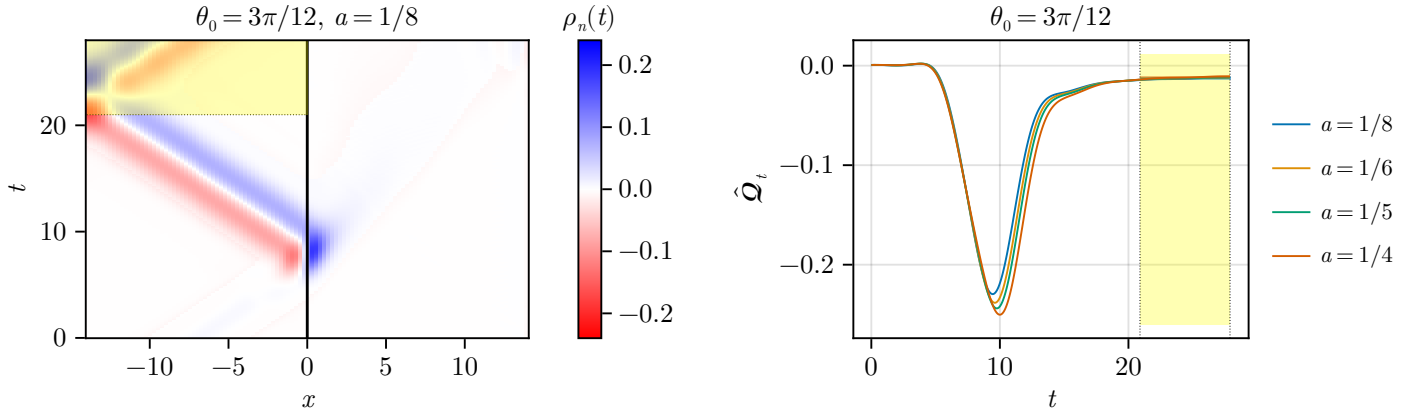

There is still significant asymmetry reflected in the displacement between the wavepackets — Phase asymmetry is a better observable at larger θ_0!

Phase Asymmetry

We show that the phase asymmetry is related to the product of the particle and anti-particle number densities in the following way:

$$-\int_{-\infty}^{0} dx\, \rho_+\, \rho_- = A\, e^{-B\Phi^2}$$

which can be used to derive Φ from the measurement of $\rho_\pm$.

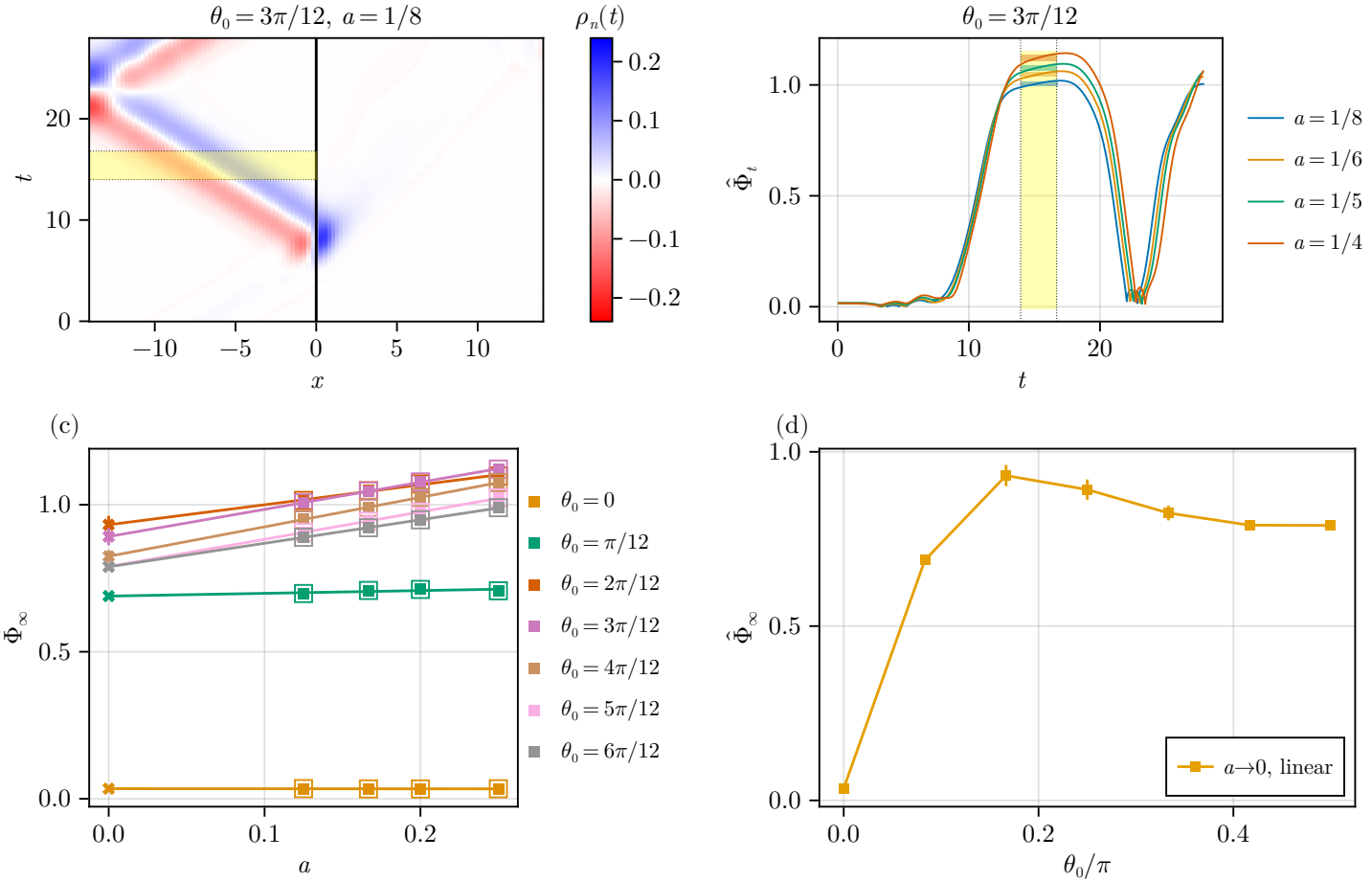

Summary

- We perform a real-time lattice simulation of fermion-bubble scattering during a first order phase transition by which the fermion obtains a complex mass in 1+1D. We analyze the symmetry breaking in different dimensions and propose the appropriate observables.
- We perform simulations with different lattice spacings and extrapolate to the continuum limit. In the real mass case, the continuum limit of the reflection coefficient agrees very well with the analytic prediction, validating our simulation.
- In the complex mass case, we define the observables that can capture the asymmetries in the magnitude and the phase of the reflection coefficient, respectively. In the scenario of equally strong reflections of both particle and anti-particle, magnitude asymmetry would be suppressed and become less sensitive, and thus it would be important to measure phase asymmetry.

Finite Volume Effects

While lattice artifacts have been eliminated by continuum limit extrapolation, finite volume effects remain as the dominant source of error until a systematic infinite volume extrapolation is performed. In our work, we investigated the performance of a simple linear extrapolation.
Magnitude and phase asymmetries in the initial state:

$L_w = 0.6,\ m_0 = 1.0,\ \theta_0 = \pi/3,\ k_0 = 1.0$

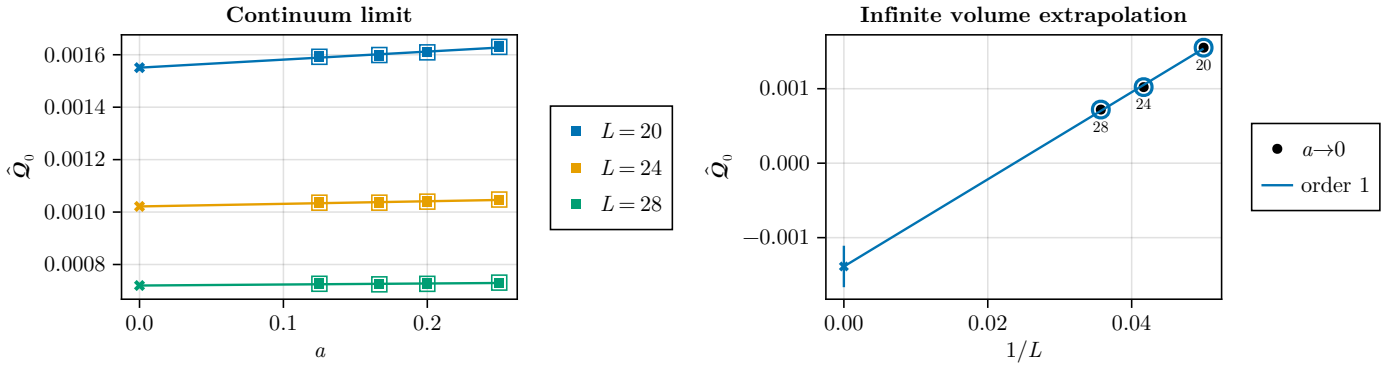

$L_w = 0.6,\ m_0 = 1.0,\ \theta_0 = \pi/3,\ k_0 = 1.0$

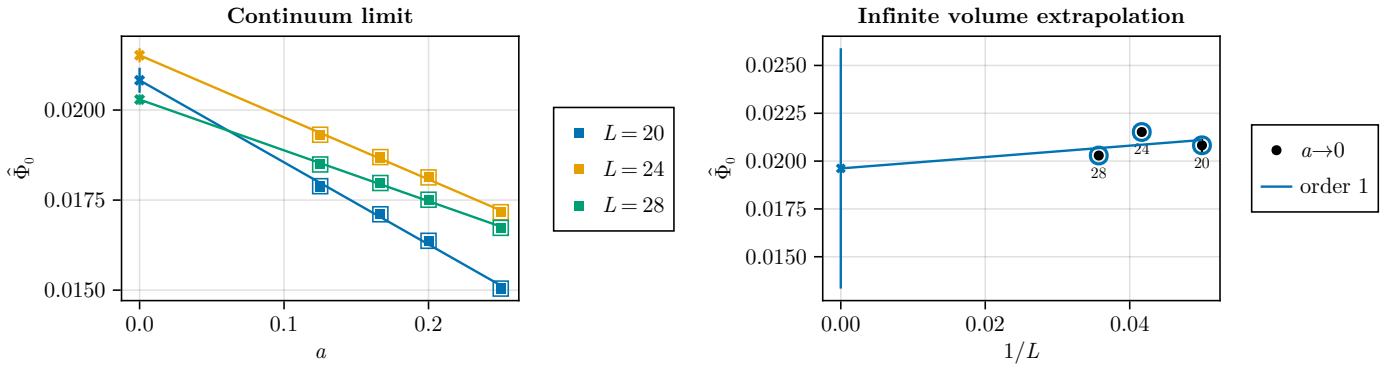

Finite Volume Effects

To investigate the finite volume effects in scattering, we take the mass profile to be a step function:

$$|m(x)| = \begin{cases} 0 & x \leq 0 \\ m_0 & x > 0 \end{cases}, \quad \theta(x) = \begin{cases} 0 & x \leq 0 \\ \theta_0 & x > 0 \end{cases}.$$

No asymmetry is expected to be generated in this case since the phase in the broken phase can be rotated away.

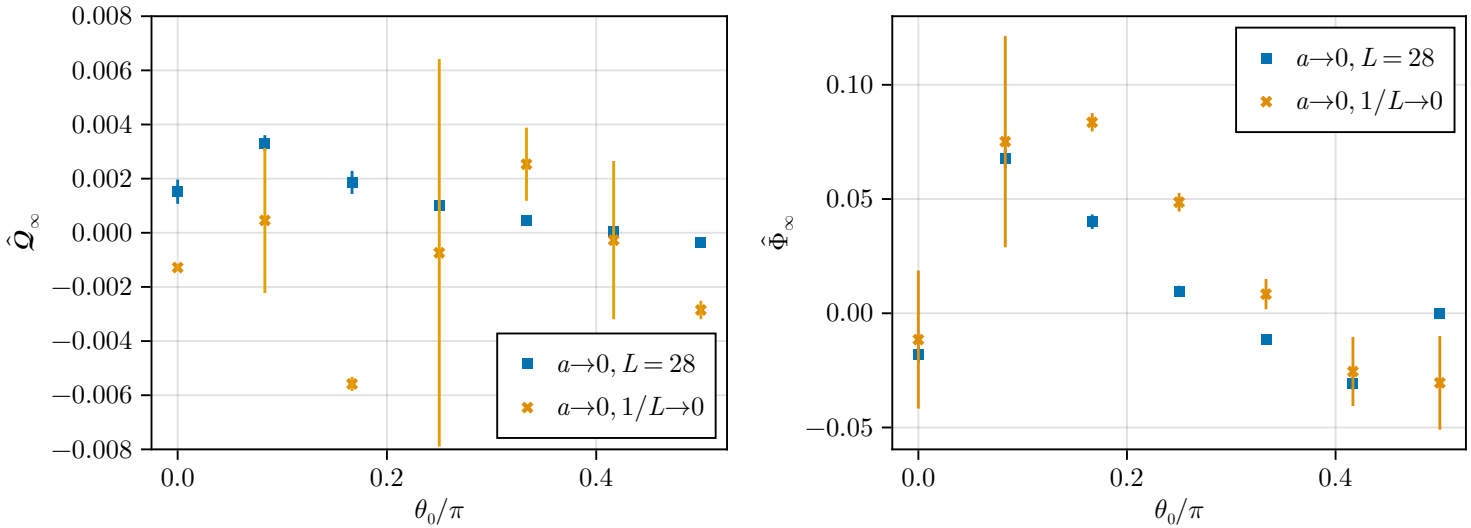

Asymmetries generated from scattering with a step mass profile. Comparing the fixed volume result with the linear infinite volume extrapolation. We see that a simple linear fit is not well under control, sometimes would produce larger uncertainties.

Outlooks

- The scalar field is treated as a static background instead of a dynamic field in this work. In the future, it will be meaningful to include the scalar field dynamics and study the full phase transition/bubble expansion dynamics.
  Real-time simulations of bubble dynamics: A. Milsted, J. Liu, J. Preskill, G. Vidal, 2012.07243, R. G. Jha, A. Milsted, D. Neuenfeld, J. Preskill, P. Vieira, 2411.13645
- This work studies a single particle dynamics in a background field, and serves as a proof of principle for future simulations in a thermal background and out-of-equilibrium environments.
  Possible strategy: Encode the thermal background into the Lindblad operators like in W. A. de Jong, K. Lee, J. Mulligan, M. Płoskoń, F. Ringer, X. Yao, 2106.08394

Real-Time Simulation of the Full EWBG

Sphaleron and phase transition involve thermal effects and should be analyzed with thermal field theory. The analysis of thermal field theory is much simplified in thermal equilibrium, where KMS condition implies a periodicity in Euclidean time $t_E = T^{-1}$. Therefore, after a Wick rotation, the time integral can be taken out from the integrated variables, such as free energy and action, leaving a purely spatial problem.

- Analytic calculation of electroweak sphaleron V.A. Kuzmin, V.A. Rubakov, M.E. Shaposhnikov, 85

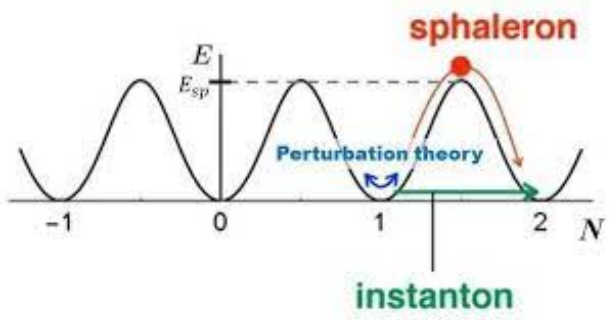

Assuming thermal equilibrium, find the field configuration $(A_{\rm cl}, \varphi_{\rm cl})$ that extremizes the static free energy

$$F = \int d^3x \left[-\frac{g_W^2(T)}{2} \mathrm{Tr}\, F_{ij}^2 + (D_i\varphi)^\dagger (D_i\varphi) + \lambda(T) \left(\varphi^\dagger\varphi - \frac{v^2(T)}{2} \right)^2 \right]$$

The free energy of this configuration is

$$F \sim 2M_W(T)/\alpha_W(T)\, B(\lambda(T)/\alpha_W(T))$$

where $B(\lambda, \alpha_W) \sim \mathcal{O}(1)$. The sphaleron rate is $\Gamma_{\rm sph} \sim \exp(-F/T)$.

Real-Time Simulation of the Full EWBG

- Analytic calculation of nucleation rate M. Dine, R. G. Leigh, P. Huet, A. Linde, D. Linde, 92
  Again due to the periodicity in thermal equilibrium, the tunneling rate $\sim \exp(-S_4) \simeq \exp(-S_3/T)$. So the critical bubble profile $\varphi(r)$ which will expand and convert the false vacuum into true vacuum is found by extremizing the 3D action

$$S_3 = 4\pi \int_0^\infty dr\, r^2 \left[\frac{1}{2} \left(\frac{d\varphi}{dr} \right)^2 + V(\varphi(r), T) \right]$$

  The nucleation temperature is usually defined as that with $S_3/T \sim 140$, when there is one bubble nucleated per Hubble time per Hubble volume.

- Effective potential
  In thermal equilibrium, the Fourier transform of the periodic correlation function has discrete frequency spectrum — Matsubara modes $\omega_n = 2n\pi T$. The thermal contribution to the effective potential is a summation over the Matsubara modes

$$V_1^T(\varphi_c) = \frac{T}{2} \sum_{n=-\infty}^{\infty} \int \frac{d^3p}{(2\pi)^3} \log \left[\omega_n^2 + p^2 + m^2(\varphi_c) \right]$$

  which enters the effective potential commonly used for EWPT calculation, $V_{\text{eff}}(\varphi, T) = V_0 + V_{\text{CW}} + V_1^T$.

Real-Time Simulation of the Full EWBG

Nearly all the analytic calculations in EWBG are based on the assumption of thermal equilibrium, despite the out-of-equilibrium nature of EWBG! To what extent are they reliable? — Real-time lattice simulation will give the final answer.

- Real-time simulation of false vacuum decay rate, e.g., D. Pîrvu, A. Shkerin, S. Sibiryakov, 2407.06263, reveals out-of-equilibrium effects during bubble nucleation.
- Real-time simulation of sphaleron rate, e.g., J. Ambjorn, T. Askgaard, H. Porter, M.E. Shaposhnikov, 90 (didn't include fermions), D. Grigoriev, M. Shaposhnikov, N. Turok, 91, A. Kovner, A. Krasnitz, R. Potting, 9907381 (included fermions).
  What's next? Sphaleron rates in general out-of-equilibrium environments?
- CP asymmetry generation in fermion-bubble scattering: Our work.
  Next: Develop the simulation in a thermal environment (in progress with Vincenzo Cirigliano, Marcela Carena and Hersh Singh). Include the scalar field and gauge field dynamics. Couple the asymmetry to the sphaleron...
  One possible toy model for a full simulation of EWBG: Abelian Higgs model coupled to fermions in 1+1D D. Grigoriev , M. Shaposhnikov, N. Turok, 92.

Thanks!